EVALUATION OF STATIC STRENGTH IN ADHESIVELY BONDED JOINTS

Tokyo Metropolitan University Student Member ○Visal Thay
Tokyo Metropolitan University Regular Member Hitoshi Nakamura
Kansai University Regular Member Toshiyuki Ishikawa
Konishi Co.,Ltd Regular Member Hisakazu Horii

1. INTRODUCTION

Recently, externally bonded patch plates, CFRP laminates (JSCE ed. (2013)) for instance, have proven to be effective for repairing or strengthening steel structures. However, debonding from the end of patch plates is one of the major concerns in application. Regarding to this problem, failure criterion for the debonding of adhesive has been studied and verified as seen in Shimizu *et al.* (2015). In this paper, toward the repair design method and data accumulation, debonding strength of two types of adhesives under principal stress failure criterion is experimentally verified and further developed.

2. EXPERIMENTAL SPECIMEN AND METHOD

2.1 Specimens and experimental series

In consideration of specimen preparations, evaluation methods and ranges, 3 test methods, a) single patch under bending moment (SPB), b) double strap under tensile force (DST) and c) single lap under tensile force (SLT), were selected. Fig. 1 shows each specimens and strain gauge position. Two types of epoxy resin were used as adhesive, Konishi E250 and Konishi E258R. Material properties of steel plate and epoxy resins are given in Table 1. Before bonding, the surfaces of the steel and patch plates were blasted by alumina and cleaned by acetone, and after bonding the specimens were cured at 40 °C for 24 hours. The thickness of adhesive was controlled to be approx. 0.4 mm using glass beads. Table 2 and Fig. 2 show the experimental series and setup of each test methods. The specimens were subjected to static load under displacement control with the speed of 5 and 2 mm/min for bending test (SPB) and tensile test (DST and SLT), respectively. In DST, the below end of the patch plates were fixed by fixture in order to control and observe the debonding at the upper end of the patch plates. The adhesive debonding was additionally observed at one side of the specimen utilizing the digital microscope with the speed of 1 frame per second, the same as the speed of load and strain data measurement.

2.2 Evaluation method

In this study, due to occurrence of high shear stress and normal stress at the end of patch plates, debonding strength is considered to be evaluated in the function of principal stress σ_{pe} given by Eq. (1).

$$\sigma_{pe} = \frac{\sigma_{ye}}{2} + \sqrt{\left(\frac{\sigma_{ye}}{2}\right)^2 + \tau_e^{\ 2}} \qquad (1)$$

Here, σ_{ye} and τ_e are normal stress and shear stress in adhesive at patch plate end which are calculated using the convergence equations (JSCE ed. (2013) and Sakamoto *et al.* (2016)).

3. EXPERIMENTAL RESULTS AND DISCUSSIONS

3.1 Test method a) SPB

Fig. 3 shows an example of the relationship between bending load and strain value obtained from strain gauge attached on patch plate at distance of 5 mm from the end of patch plate. In this test method, the debonding load is extracted where strain values returned to zero, (considered as complete debonding), instead of maximum strain values

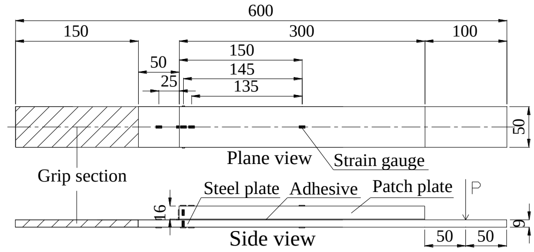

(a) Single Patch – Bending (SPB)

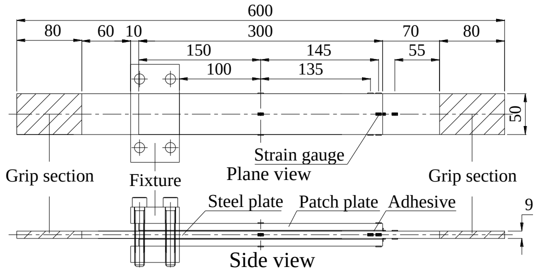

(b) Double Strap – Tensile (DST)

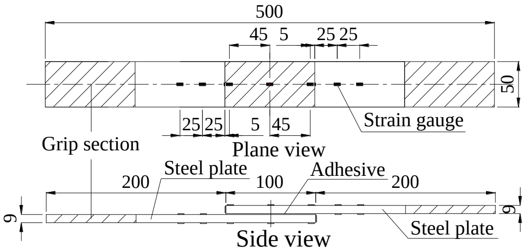

(c) Single Lap – Tensile (SLT)

Fig. 1 Experimental specimen and strain gauge position

Table 1 Material properties

Materials	Elastic modulus E (GPa)	Poisson's ratio ν	Yield Strength σ_y (MPa)	Tensile Strength σ_{tu} (MPa)
Steel plate (SM490YA)	210	0.28	410	554
Adhesive (Konishi E250)	2.6	0.34	–	25
Adhesive (Konishi E258R)	3.6	0.34	–	33

Table 2 Experimental series

Test name	Specimen series	Adhesive type	Base plate thickness t_b (mm)	Patch plate thickness t_p (mm)	Number of test pieces
Single Patch - Bending (SPB)	E250P16, 4.5	E250	9	16, 4.5	3, 3
	E258RP9, 4.5	E258R	9	9, 4.5	3, 3
Double Strap - Tensile (DST)	E250P16	E250	9	16	3
	E258RP16	E258R	9	16	3
Single Lap - Tensile (SLT)	E250P9	E250	9	9	3
	E258RP9	E258R	9	9	3

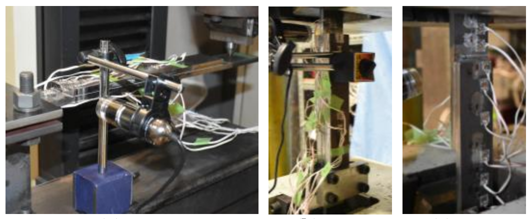

(a) SPB **(b)** DST **(c)** SLT

Fig. 2 Test setup

Keywords: Adhesive joint, Adhesive debonding, Static strength, Principal stress, Failure criterion
Contact address: Minami-Osawa 1-1, Hachioji-shi, Tokyo, 192-0397, Japan, Tel: +81-42-677-1111, Ext. 4564

(considered as initial debonding). Fig. 4 shows debonding image at patch plate end taken at maximum strain and at where the debonding is visually confirmed via microscope. From the figure, the debonding cannot be confirmed at maximum strain (Fig. 4(a)). However, load at visual debonding (Fig. 4(b)) is very close to load at zero strain as plotted in Fig. 3. For test No. 1, the debonding load is obtained from strain value at 15 mm instead of 5 mm due to failure of strain gauge.

3.2 Test method b) DST

Fig. 5 shows the relationship between tensile stress and strain value obtained from strain gauge attached on patch plate (debonding side) at distance of 5 mm from the end of patch plate for E250 and E258R. Fig. 6 shows the debonding image at patch plate end taken at where the debonding is visually confirmed via microscope for E250 and E258R. In case of E250, strain value returned zero shortly after maximum strain as seen in Fig. 5 and debonding is visually confirmed at zero strain. Therefore, the debonding load of E250 is extracted at zero strain. In case of E258R, strain value is quickly dropping to zero after maximum strain. This sudden drop might be reasoned from yield of steel base plate. In this case, the debonding load at maximum strain was chosen as visual debonding was confirmed before zero strain and shortly after the maximum strain.

3.2 Test method c) SLT

In this test method, due to complete failure of specimen occurred at the time or immediately after the debonding of adhesive, maximum load is considered as debonding moment. In theoretical calculation process of shear stress and normal stress of adhesive (Sakamoto *et al.* (2016)), the non-adhered length of specimen is recalculation due to the occurrence of bending moment at grip section where the boundary condition of test setup is fixed end. Fig. 7 show an example of bending moment diagram at the debonding. The experimental bending moment is obtained from strain gauge attached at the distance of 50 and 75 mm from each grip sections. From the figure, bending moment is zero at 13 mm from grip section and non-adhered length is 13 mm shorter than the actual length.

3.2 Failure criterion

Fig. 8 plotted all and average experimental values of principal stress at debonding of each test methods and the failure envelopes based on principal stress criterion of E250 and E258R. The failure envelopes are obtained from Eq. (1) where the principal stress of E250 and E258R are 44.4 and 115.9 MPa, respectively. From the figure, the experimental data has been fitted to the failure criterion for either E250 or E258R. The coefficients of variation of E250 and E258R are 0.18 and 0.10, respectively, and all data are above -1.64σ (σ: standard deviation). The principal stress at debonding of E258R is relatively larger than that of E250, accounting about 2.61 times. Moreover, this ratio based on debonding principal stress is much more larger than that of tensile strength from material test as shown in Table 1 (E250:E258R=1:1.32).

4. CONCLUSIONS

In conclusion, the experimental data of each test methods has been fitted to the failure criterion based on principal stress for either E250 or E258R. The ratio under principal stress of E258R and E250 is approx. 2.61, larger compared to the ratio under tensile strength. Future work deals with relationship of this ratio to simplify the evaluation method by taking into account failure mechanism or adhesive characteristics.

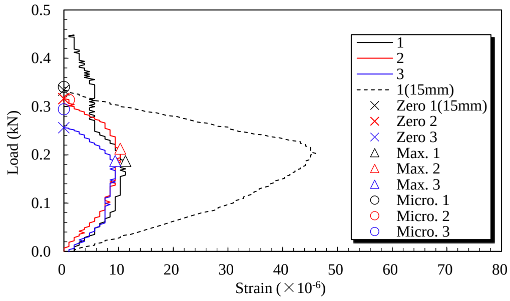

Fig. 3 Load – strain near patch plate end (SPB_E250P16)

(a) Image at maximum strain **(b)** Image at debonding

Fig. 4 Debonding image at patch plate end (SPB_E250P16-1)

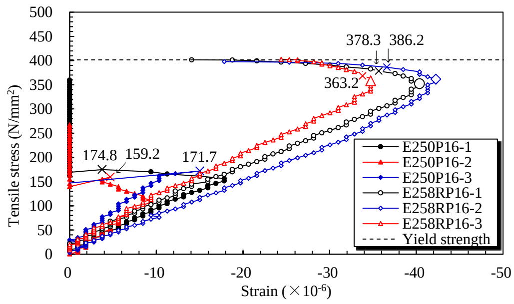

Fig. 5 Tensile stress – strain near patch plate end (DST_E250P16 and DST_E258RP16)

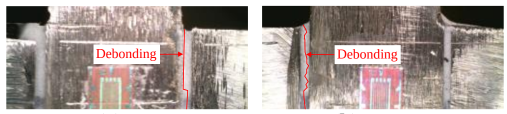

(a) E250 **(b)** E258R

Fig. 6 Debonding image at patch plate end (DST)

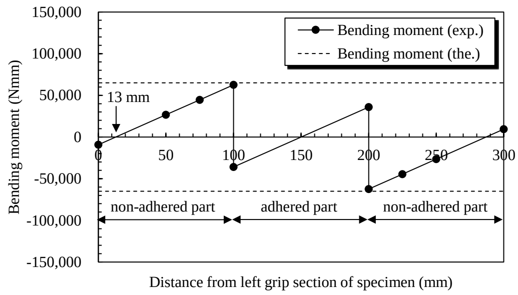

Fig. 7 Bending moment at debonding (SLT_E250P9-1)

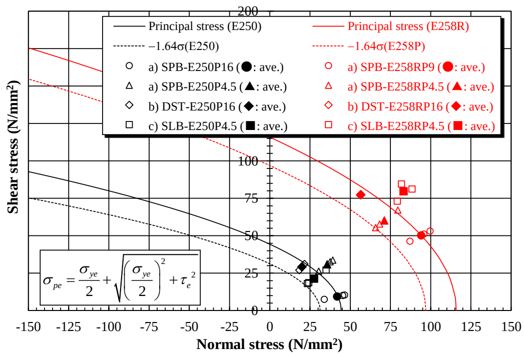

$$\sigma_{pe}=\frac{\sigma_{ye}}{2}+\sqrt{\left(\frac{\sigma_{ye}}{2}\right)^2+\tau_e^2}$$

Fig. 8 Failure envelopes based on principal stress criterion

REFERENCES

Japan Society of Civil Engineers: Advanced Technologies of Joining for FRP Structures and FRP Bonding for Steel Structures, Hybrid Structure Report 09, 2013. [in Japanese]

Shimizu M., Ishikawa T., Horii H., Hattori A., and Kawano H.: Evaluation for Debonding of Patch Plate Bonded to Butted Steel Plates, Journal of Steel Construction, JSSC, Vol.22-86, 2015. [in Japanese]

Sakamoto T. and Ishikawa T.: Theoretical Analysis of Single Lap Adhesive Joint and Energy Release Rate for Debonding, Journal of JSCE, Vol.72-2, 2016, pp. I_653-I_662. [in Japanese]